http://dx.doi.org/10.5012/bkcs.2011.32.9.3223

# Emission Detection of Mercuric Ions in Aqueous Media Based-on Dehybridization of DNA Duplexes

**Byul Nim Oh, Qiong Wu, Mi Sun Cha, Hee Kyung Kang, Jin Ah Kim, Ka Young Kim, Eswaran Rajkumar, and Jinheung Kim***

*Department of Chemistry and Nano Science, Ewha Womans University, Seoul 120-750, Korea. *E-mail: jinheung@ewha.ac.kr*
*Received June 8, 2011, Accepted July 12, 2011*

To quantify the presence of mercuric ions in aqueous solution, double-stranded DNA (dsDNA) of poly(dT) was employed using a light switch compound, $Ru(phen)_2(dppz)^{2+}$ (**1**) which is reported to intercalate into dsDNA of a right-handed B-form. Addition of mercuric ions induced the dehybridization of poly(dT)·poly(dA) duplexes to form a hairpin structure of poly(dT) at room temperature and the metal-to-ligand charge transfer emission derived from the intercalation of **1** was reduced due to the dehybridization of dsDNA. As the concentration of $Hg^{2+}$ was increased, the emission of **1** progressively decreased. This label-free emission method had a detection limit of 0.2 nM. Other metal ions, such as $K^+$, $Ag^+$, $Ca^{2+}$, $Mg^{2+}$, $Zn^{2+}$, $Mn^{2+}$, $Co^{2+}$, $Ni^{2+}$, $Cu^{2+}$, $Cd^{2+}$, $Cr^{3+}$, $Fe^{3+}$, had no significant effect on reducing emission. This emission method can differentiate matched and mismatched poly(dT) sequences based on the emission intensity of dsDNA.

**Key Words :** Metal-to-ligand transfer emission, DNA intercalation, Poly(dT), Mercuric ion sensing, Light switch Ru compound, Mismatch detection

## Introduction

Mercuric ions are a highly toxic and acts as severe environmental pollutant that have serious medical effects on human beings.[1-3] While solvated mercuric ions in aqueous media are caustic and carcinogenic with high cellular toxicity, methyl mercury which is produced by microbial biomethylation of mercuric ions can accumulate in the human body through the food chain and cause serious and permanent brain damage and other chronic diseases.[4-6] It is also important to control the leakage of mercuric ions from amalgam fillings during dental care.[7] Therefore, routine detection of $Hg^{2+}$ with high sensitivity and selectivity is central to the environmental monitoring of river, sewage, etc., and for evaluating the safety of food supplies.[8-11] Several photoemission methods for the detection of $Hg^{2+}$ have been developed based on organic molecules,[8,12-17] oligonucleotides,[18,19] proteins,[20] and conjugated polymers.[21,22] Although some sensors displayed a high enough sensitivity and selectivity for detection of mercuric ions in aqueous solution, the preparation and operation of these devices were quite needy and these sensors could not be easily operated onsite for real-time detection as well as quantification. Therefore, simple assay methods with respect to sensitivity and selectivity with aqueous environments are still needed for routine and real-time mercury detection.

Oligonucleotides provided a charming methodology for $Hg^{2+}$ sensing in aqueous solution. DNA-based detection systems can be used for this purpose since $Hg^{2+}$ has been shown to specifically coordinate to two DNA thymine bases (T) and stabilize T–T mismatches in DNA duplexes.[18,23-30] Thymine-rich nucleic acids separated by a spacer and tethered with fluorophore/quencher units at their ends were developed to analyze $Hg^{2+}$ ions by the ion-induced formation of a hairpin structure, yielding an intramolecular fluorescence resonance energy transfer process.[19] Recently, DNA-gold nanoparticles (AuNPs) were used for the detection of $Hg^{2+}$ through colorimetric methods as AuNPs have unique extinction coefficients.[25,29,30] The colorimetric detection method for $Hg^{2+}$ using T- $Hg^{2+}$-T coordination and Au nanoparticles had a limit of detection close to 100 nM; however, this sensor required thiolated oligonucleotides and an additional step to prepare the DNA-AuNP aggregates.[29] Another different method was reported based on $Hg^{2+}$-induced aggregation of AuNPs of which surface was stabilized by a single-stranded thymine-rich DNA strand.[25]

Polypyridine ruthenium complexes and their interactions with oligonucleotides have been extensively studied due to their interesting properties derived from emission via metal-to-ligand charge transfer (MLCT). Especially, $Ru(phen)_2(dppz)^{2+}$ (**1**) (phen = 1,10-phenanthroline, dppz = dipyrido-[3,2-*a*:2',3'-*c*]phenazine) which selectively intercalates into the right-handed B-form double-stranded DNA, has been frequently used to study electron transfer through DNA duplexes and to analyze DNA by utilizing the emission enhancement when **1** was intercalated within the base pairs of DNA duplexes.[31-33] Recently, we developed a label-free assay for potassium ions and target oligonucleotides containing single-base mismatches using a $K^+$-specific aptamer and $Ru(phen)_2(dppz)^{2+}$.[34] Here, we introduce a new homogeneous assay using double-stranded poly(dT)/poly(dA) utilizing the intercalation property of **1** for the selective and sensitive assay of mercuric ions using the metal ion-induced formation of a hairpin structure. Using this approach, the amount of **1** intercalated into double-stranded DNA can be used to quantify the mercuric ion concentration since dsDNA is dehybridized and converted to the hairpin structure in the presence of mercuric ions. In addition, the decreasing rates of emission by dehybridization allowed us to differentiate matched and mismatched sequences. The high sensitivity of 0.2 nM was obtained due to the use of the strong emission enhancement because several molecules of **1** can be intercalated into dsDNA.

## Results and Discussion

The coordination compound Δ-Ru(phen)$_2$(dppz)$^{2+}$ (**1**) has been reported to intercalate among alternate base pairs double-stranded nucleic acids (dsDNA).[32,33,35,36] Upon intercalation of **1** into dsDNA, a strong MLCT emission occurring in the hydrophobic environment is generated relative to no emission of **1** alone in aqueous solution. In this study, dsDNA prepared with 22-mer oligonucleotides, poly(dT)$_{22}$ (T$_{22}$) and poly(dA)$_{22}$ (A$_{22}$), was used to detect mercuric ions through the emission measurements (Figure 1). When 0.10 μM T$_{22}$·A$_{22}$ was treated with 4.0 μM **1** in Na-phosphate buffer (pH = 7.0), a strong emission enhancement was observed (Figure 2). Since **1** is reported to intercalate into the alternate base pairs of dsDNA, the emission intensity obtained with 40 equiv **1** corresponds to the maximum which can be obtained with T$_{22}$·A$_{22}$ . A hairpin structure of T$_{22}$ was then generated from T$_{22}$ upon treatment with 50 equiv $Hg^{2+}$. The emission intensity in the presence of the hairpin structure generated in the presence of $Hg^{2+}$ was drastically lower than with T$_{22}$·A$_{22}$. When T$_{22}$·A$_{22}$ was treated and incubated with 50 equiv $Hg^{2+}$ for 10 min at room temperature, the emission intensity of **1** also was reduced rapidly relative to that obtained with T$_{22}$·A$_{22}$ alone. The emission intensity obtained with T$_{22}$·A$_{22}$ and $Hg^{2+}$ was close

| | |
|---|---|
| A$_{22}$ | 5' -AAA AAA AAA AAA AAA AAA AAA A |
| T$_{22}$ | 5'-TTT TTT TTT TTT TTT TTT TTT T |
| T$_{21}$G | 5'-TTT TTT TTT TGT TTT TTT TTT T |
| T$_{21}$C | 5'- TTT TTT TTT TCT TTT TTT TTT T |
| T$_{21}$A | 5'- TTT TTT TTT TAT TTT TTT TTT T |

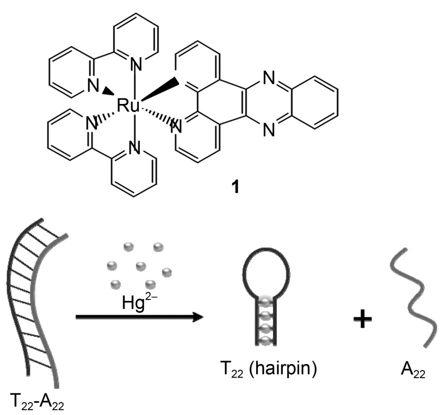


**Figure 1.** Sequences of the oligonucleotides used in this study, and a schematic representation of label-free fluorescent detection of mercuric ions using dsDNA and Δ-Ru(phen)$_2$(dppz)$^{2+}$ (**1**).

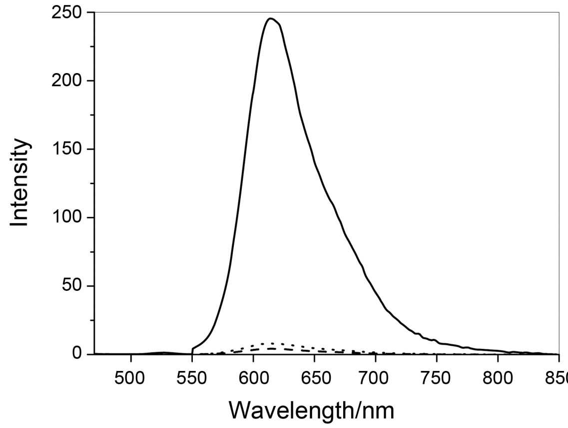


**Figure 2.** Emission spectra ($\lambda_{ex}$ = 480 nm) of **1** (4.0 μM) for 0.10 iM T$_{22}$·A$_{22}$ (—), 0.10 μM T$_{22}$ (---), and 0.10 μM T$_{22}$·A$_{22}$ treated with 10 equiv $Hg^{2+}$ (···) in 10 mM phosphate buffer (pH = 7.0) at room temperature.

to that obtained with the hairpin structure of T$_{22}$ generated from T$_{22}$ upon treatment with 10 equiv $Hg^{2+}$. As a control experiment, G$_{22}$·C$_{22}$ was used in place of T$_{22}$·A$_{22}$ under the same conditions. Interestingly, the emission intensity of **1** with G$_{22}$·C$_{22}$ alone was much lower than that with T$_{22}$·A$_{22}$ and the intensity changed slightly upon treatment with 10 equiv $Hg^{2+}$ to G$_{22}$·C$_{22}$ (Figure 3). For another control experiment, ethidium bromide which is also a well known DNA-intercalating agent was tested instead of **1** in the same assay with T$_{22}$·A$_{22}$, but such significant emission changes were not observed in the treatment with $Hg^{2+}$ under the same reaction conditions (Figure 4).

The emission spectra of the **1**-T$_{22}$·A$_{22}$ sensing system were obtained at different $Hg^{2+}$ concentrations (Figure 5(a)). The emission intensity of **1** decreased at increasing $Hg^{2+}$ concentrations. The emission almost disappeared at about 50 equiv $Hg^{2+}$, indicating that the 50 equiv is required to afford the full formation of the hairpin conformation of T$_{22}$ from the dehybridization of T$_{22}$·A$_{22}$ through T-$Hg^{2+}$-T coordination. The calibration curve corresponding to the emission changes

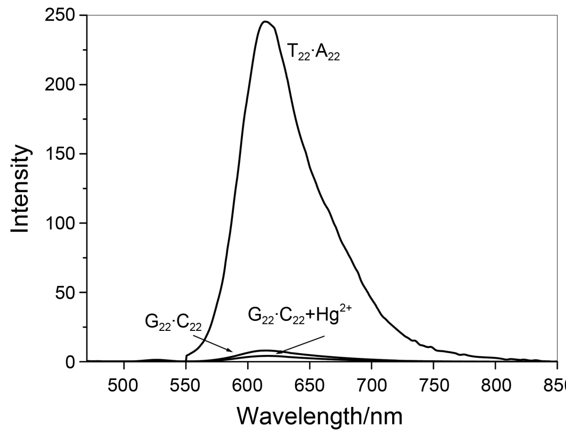


**Figure 3.** Emission spectra of **1** in the presence of 0.10 μM G$_{22}$·C$_{22}$ without and with 10 equiv $Hg^{2+}$ in phosphate buffer (pH = 7.0). These emission spectra were plotted together with that of T$_{22}$·A$_{22}$ for comparison.

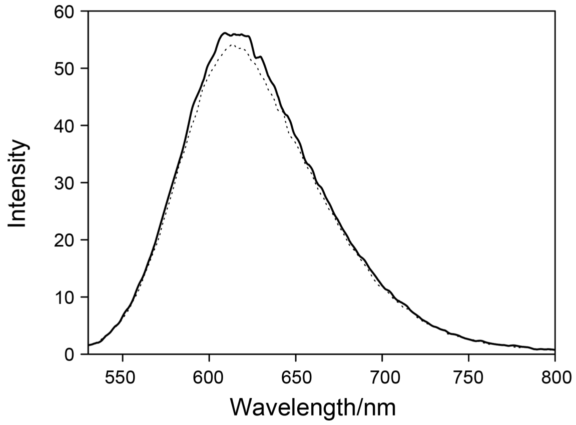


**Figure 4.** Emission emission spectra ($\lambda_{ex}$ = 510 nm) of ethidium bromide in the presence of 0.10 μM $T_{22}{\cdot}A_{22}$ (solid) and 0.10 μM $T_{22}{\cdot}A_{22}$ treated with 10 equiv $Hg^{2+}$ (dotted).

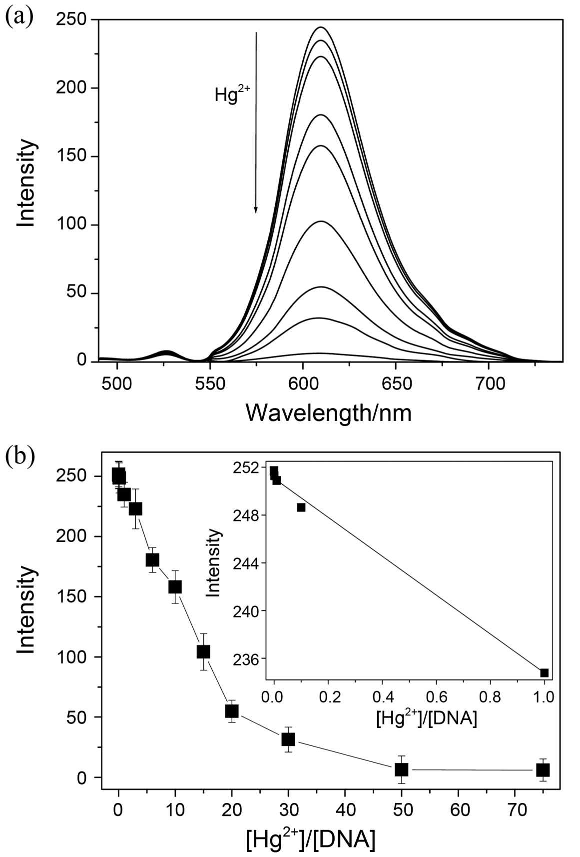


**Figure 5.** (a) Emission spectra of **1** at different concentrations of $Hg^{2+}$ in the presence of $T_{22}{\cdot}A_{22}$ (0.10 μM) in 10 mM phosphate buffer. (b) Plot of intensity against the concentration of $Hg^{2+}$. Samples were analyzed at 615 nm ($\lambda_{ex}$ = 480 nm).

in the sensing system at different $Hg^{2+}$ concentrations is shown in Figure 5(b). Thus, the difference in emission intensity of **1** upon addition of $Hg^{2+}$ could be used to measure $Hg^{2+}$ at concentrations ranging from 1 nM to 50 μM which is the widest range among the $Hg^{2+}$-sensing methods reported ever. The detection limit of the sensor using $T_{22}{\cdot}A_{22}$ was about 0.2 nM.

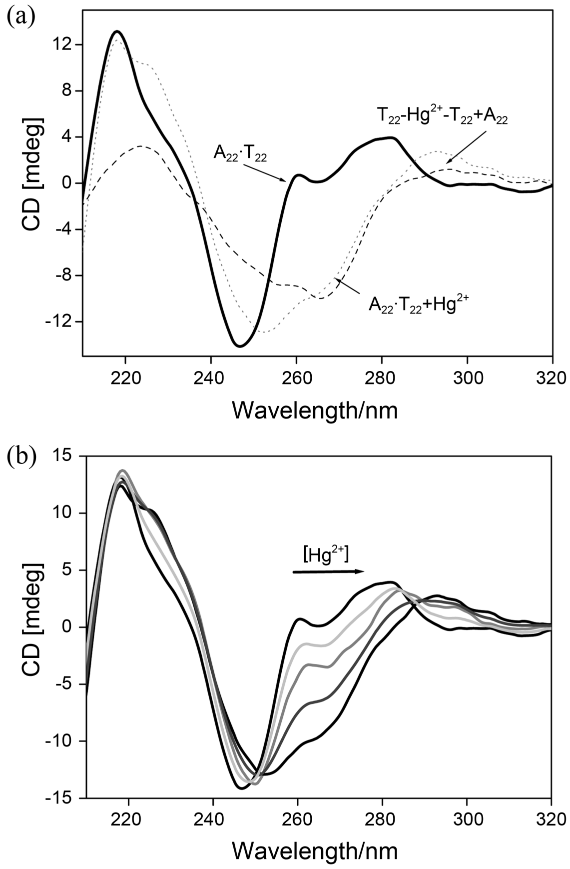


**Figure 6.** (a) Circular dichroism spectra of 1.0 μM $T_{22}{\cdot}A_{22}$, $T_{22}{\cdot}A_{22}$ treated with 50 equiv $Hg^{2+}$, and the mixture of $A_{22}$ and the hairpin structure prepared with $T_{22}$ and 50 equiv $Hg^{2+}$ in 10 mM phosphate buffer (pH = 7.0). (b) CD spectral changes of $T_{22}{\cdot}A_{22}$ upon addition of 0, 5, 10, 30, and 50 equiv $Hg^{2+}$ ions.

Single-stranded poly(dT) was well reported to form a stable hairpin conformation in the presence of $Hg^{2+}$.[19,37,38] Even, a folded G-quadruplex structure formed by binding with a hemin protein was disentangled by the formation of T-T mismatched base pairs upon addition of $Hg^{2+}$.[39] A DNA probe containing several thymine bases that was hybridized with 10 base pairs to a complementary strand was also dehybridized upon treatment with $Hg^{2+}$ to form a hairpin structure.[40] In that case, some thymine bases of the probe which are supposed to induce the formation of the hairpin structure through the $Hg^{2+}$ coordination were left without base-pairing with the complementary strand. These thymine bases left without base-pairing could activate the dehybridization of the probe upon treatment with $Hg^{2+}$. Based on the observed decrease in emission upon the addition of $Hg^{2+}$ to the fully hybridized $T_{22}{\cdot}A_{22}$, the possibility of dehybridization of the relatively long $T_{22}{\cdot}A_{22}$ was examined using circular dichroism (CD). A $T_{22}{\cdot}A_{22}$ solution upon treatment with 50 equiv $Hg^{2+}$ afforded a positive ellipticity in the CD spectrum at 290 nm which presents a striking contrast to the 260 and 280 nm band obtained with $T_{22}{\cdot}A_{22}$ (Figure 6(a)). The positive band at 290 nm was also observed in the mixture of $A_{22}$ and the hairpin form prepared with $T_{22}$ and

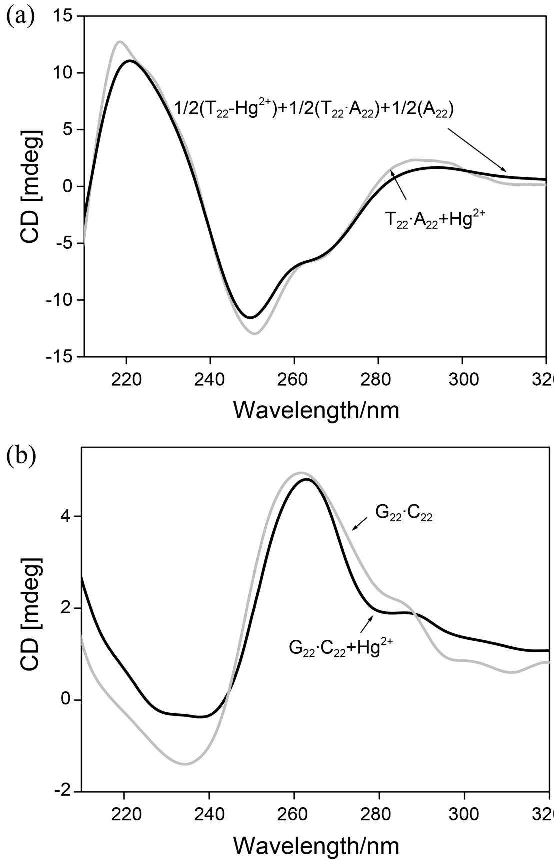


**Figure 7.** (a) Circular dichroism spectra collected with 1.0 μM $T_{22}\cdot A_{22}$ treated with 15 equiv $Hg^{2+}$ (gray line) and the mixture of 0.5 μM $T_{22}\cdot A_{22}$ + 0.5 μM $A_{22}$ + the hairpin structure prepared with 0.5 μM $T_{22}$ and 15 equiv $Hg^{2+}$ (black) in 10 mM phosphate buffer (pH = 7.0). (b) Circular dichroism spectra collected with 1.0 μM $G_{22}\cdot C_{22}$ (gray line) and 1.0 μM $G_{22}\cdot C_{22}$ treated with 25 equiv $Hg^{2+}$ (black) in 10 mM phosphate buffer (pH = 7.0).

50 equiv $Hg^{2+}$, indicating that $T_{22}\cdot A_{22}$ was in fact dehybridized upon addition of $Hg^{2+}$. When $T_{22}\cdot A_{22}$ was titrated with 10, 20, 30, and 50 equiv $Hg^{2+}$, the positive band of $T_{22}\cdot A_{22}$ at 260 nm was gradually shifted to that at 290 nm (Figure 6(b)). This progressive shift demonstrates that a certain amount of $T_{22}$ exists in the hairpin form due to $Hg^{2+}$ treatment and the rest remains still in the double stranded form. For example, when a sample was treated with 10 equiv $Hg^{2+}$, about 30% of the $T_{22}\cdot A_{22}$ was dehybridized to produce the hairpin form, resulting in the corresponding emission intensity shown in Figure 5. In addition, the CD spectrum of 1.0 μM $T_{22}\cdot A_{22}$ upon treatment with 15 equiv $Hg^{2+}$ was very similar to that of the mixture of 0.5 μM $T_{22}\cdot A_{22}$ and the hairpin form prepared with 0.5 μM $T_{22}$ and 15 equiv $Hg^{2+}$ (Figure 7(a)). Furthermore, when $G_{22}\cdot C_{22}$ was treated with 25 equiv $Hg^{2+}$, no significant change in the CD spectrum was observed (Figure 7(b)). Taken together, these data are most consistent with the dehybridization of $T_{22}\cdot A_{22}$ into the hairpin confirmation upon $Hg^{2+}$ treatment.

The selectivity of $T_{22}\cdot A_{22}$ for 50 equiv $Hg^{2+}$ was evaluated by observing the response of the assay to other relevant metal ions, such as $K^+$, $Ag^+$, $Ca^{2+}$, $Mg^{2+}$, $Zn^{2+}$, $Mn^{2+}$, $Co^{2+}$,

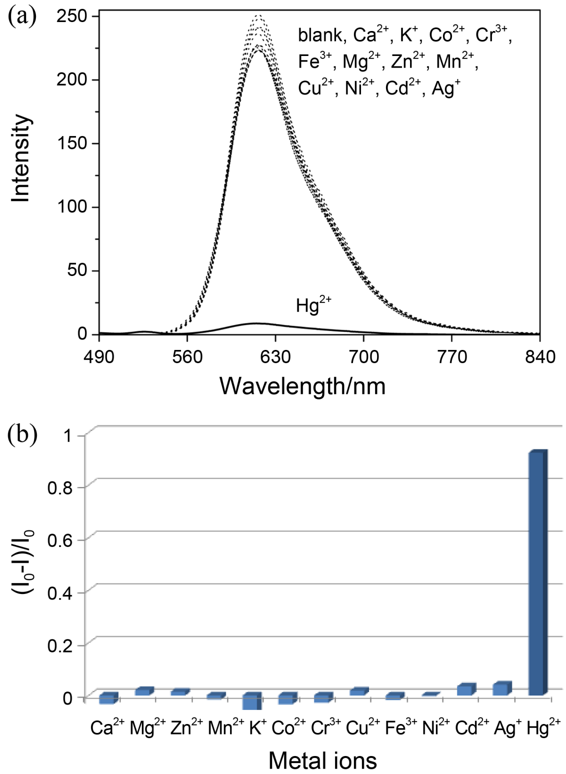


**Figure 8.** (a) Selectivity of the $Hg^{2+}$-ion sensor. The concentration of $Hg^{2+}$ was 1.0 μM and the concentration of all other metal ions was 0.1 mM. (b) Relative increase in fluorescence intensity $[(I_o-I)/I_o]$ of 10 mM phosphate solutions containing 0.10 μM $T_{22}\cdot A_{22}$ and 4.0 μM **1** upon the addition of 1.0 μM $Hg^{2+}$ or the other metal ions (0.1 mM). $I_o$ and $I$ describe the emission intensities of **1** in the absence and presence of metal ions, respectively.

$Cr^{2+}$, $Cu^{2+}$, $Ni^{2+}$, $Cd^{2+}$, and $Fe^{3+}$ at a concentration of 0.1 mM (Figure 8). Only $Hg^{2+}$ displayed a marked emission change relative to the control ions and the selectivity was determined to be at least 110000-fold higher for $Hg^{2+}$ ions over any other metal ions. In addition, when $Hg^{2+}$ (5.0 μM) and another metal ions ($M^{n+}$, 200 μM) were treated together to the $T_{22}\cdot A_{22}$ solution, the emission response of the $Hg^{2+}$-$M^{n+}$ pair was similar to with $Hg^{2+}$ alone, demonstrating excellent selectivity over other metal ions as well.

Oligonucleotides containing a single-mismatched base pair in the middle of $T_{22}$ were then examined to determine if differences in emission intensity were related to the conformational change upon treatment with $Hg^{2+}$ (Figure 9).

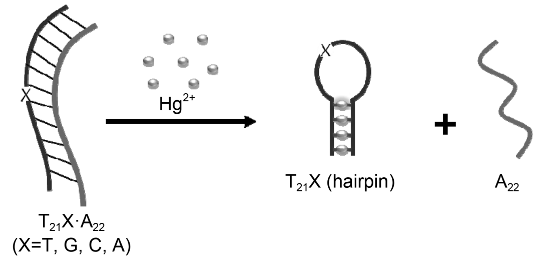


**Figure 9.** Scheme of dehybridization of matched and mismatched dsDNA upon treatment with $Hg^{2+}$ and formation of hairpin structures.

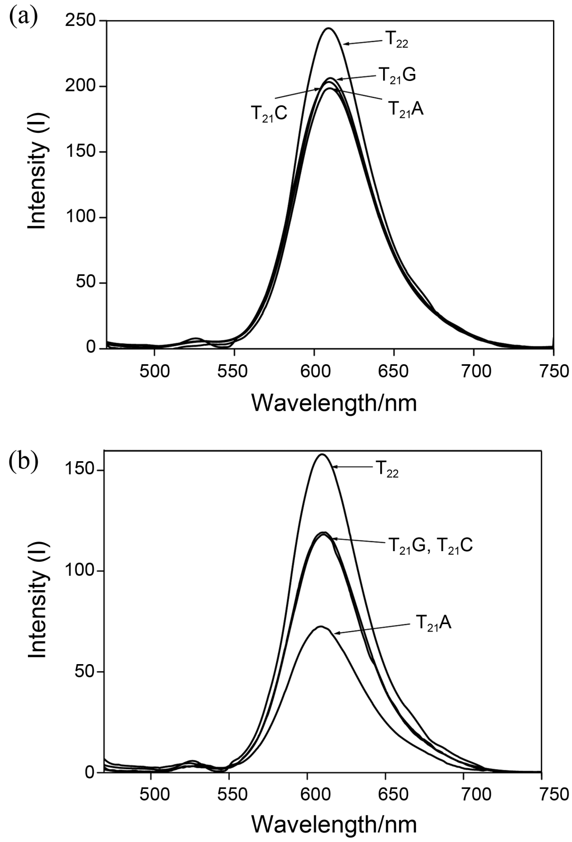


**Figure 10.** (a) Emission spectra of **1** with 0.10 μM $T_{22}$·$A_{22}$, $T_{21}G$·$A_{22}$,$T_{21}C$·$A_{22}$, and $T_{21}A$·$A_{22}$ in 10 mM phosphate buffer. (b) Emission spectra of $T_{22}$·$A_{22}$, $T_{10}G$·$A_{11}$, $T_{10}C$·$A_{11}$, and $T_{10}A$·$A_{11}$ upon treatment with 4.0 μM $Hg^{2+}$ ions.

Double-stranded DNA containing a single-base mismatched base in poly(dT), such as $T_{21}G$·$A_{22}$, $T_{21}C$·$A_{22}$, and $T_{21}A$·$A_{22}$, were tested. $T_{22}$·$A_{22}$ displayed the highest intensity relative to the mismatched (Figure 10(a)). The formation rates of the hairpin structures were expected to induce differences in the emission intensity since the dehybridization rates with the matched dsDNA could be slower than those with the mismatched dsDNA upon treatment with $Hg^{2+}$. Indeed, $T_{22}$·$A_{22}$ displayed difference in intensity relative to those of the mismatched. $T_{21}G$·$A_{22}$ and $T_{21}C$·$A_{22}$ also showed different time traces relative to $T_{21}A$·$A_{22}$ (Figure 10(b)), indicating that the dehybridization extent of $T_{21}G$·$A_{22}$ and $T_{21}C$·$A_{22}$ was relatively low. The order in the emission intensity was $T_{11}$·$A_{22}$> $T_{21}G$·$A_{22}$ = $T_{21}C$·$A_{22}$ > $T_{21}A$·$A_{22}$ demonstrating that this method was quite sensitive to distinguish the matched and mismatched dsDNA.

## Conclusions

We rationally developed a label-free emission method to detect $Hg^{2+}$ using double-stranded DNA of a poly(dT) sequence which can be intercalated by the light-switch Ru complex as an extrinsic emission reagent in aqueous media. The structural switching of dsDNA upon $Hg^{2+}$ binding provided the opportunity to tune the dynamic range of $Hg^{2+}$. A detection limit as low as 0.2 nM for $Hg^{2+}$ was obtained using this label-free emission method, which also displayed an excellent selectivity toward $Hg^{2+}$ over several other mono, di, and trivalent metal ions. The emission measurements upon treatment with $Hg^{2+}$ allowed to distinguish the matched from the mismatched dsDNA. This simple system of highly sensitive and selective sensing could apply for real-time mercuric ion detection in environmental samples and in other applications.

## Experimental Section

**Materials and Instrumentation.** All chemicals obtained from Aldrich Chemical Co. were of the best available purity and used without further purification unless otherwise indicated. The ultrapure water produced by a Millipore Elix A3-MilliQ system (MilliQ, Germany) was used to prepare the aqueous solutions. Δ-Ru(phen)$_2$(dppz)$Cl_2$ (**1**) was prepared as described elsewhere.[41] All oligonucleotides were purchased from JenoTec Inc. (Deajeon, Korea) and were purified by HPLC using a Thermo hypersyl gold column (0.46 × 25 cm). Oligonucleotide concentrations were determined spectrophotometrically by monitoring the absorbance at 260 nm on a Hewlett-Packard 8452A diode-array spectrometer. Once single-stranded DNA concentrations were known, equal molar amounts of complementary DNA were mixed, and the solution annealed at 90 °C for 5 min and then allowed to slowly cool to room temperature to prepare double-stranded DNA.

Emission spectra were collected using a Perkin-Elmer LS 55 luminescence spectrophotometer. Optical rotations were determined at ambient temperature using a JASCO J-810 polarimeter.

**Detection of Mercuric Ions.** The solution of dsDNA (0.10 μM, $T_{22}$·$A_{22}$) was treated with a predetermined amount of $Hg(ClO_4)_2$ dissolved in an aqueous solution containing 10 mM phosphate buffer (pH = 7.0) for 5 min at room temperature. Then, the solution was mixed with **1** for 1 min before measurement at room temperature. **1** and dsDNA were suspended in the same buffer so that the composition of the buffer did not change in the final solution. Experiments with the other metal ions were carried out under the same conditions. The data points were obtained from the average of three independent measurements.

**Emission Measurement with dsDNA.** In a typical experiment, a sample containing mercuric ions (1.0 or 5.0 μM) dissolved in a buffered aqueous solution containing 10 mM phosphate buffer (pH = 7.0) was mixed with 0.10 μM matched or mismatched dsDNA at room temperature. Then, **1** (4.0 μM) was treated and the emission spectra were taken after 1 min at a certain time interval.

**Acknowledgments.** This work is supported by the National Research Foundation of Korea Grant funded by the Korean Government (2010-0001485, 2009-0087304, and SRC Program: 2011-0001335), and BK21 (to B. N. O., W. Q., J.A.K., H. K. K., M.S.C., and K.Y.K.).

## References


1. Baughman, T. A. *Environ. Health Perspect* **2006**, *114*, 147.
2. Virtanen, J. K.; Rissanen, T. H.; Voutilainen, S.; Tuomainen, T.-P. *J. Nutr. Biochem.* **2007**, *18*, 75.
3. Vupputuri, S.; Longnecker, M. P.; Daniels, J. L.; Guo, X.; Sandler, D. P. *Environ. Res.* **2005**, *97*, 195.
4. Tchounwou, P. B.; Ayensu, W. K.; Ninashvili, N.; Sutton, D. *Environ. Toxicol.* **2003**, *18*, 149.
5. Onyido, I.; Norris, A. R.; Buncel, E. *Chem. Rev.* **2004**, *104*, 5911.
6. Morel, F. M. M.; Kraepiel, A. M. L.; Amyot, M. *Annu. Rev. Ecol. Syst.* **1998**, *29*, 543.
7. Halbach, S.; Kremers, L.; Willruth, H.; Mehl, A.; Elzl, G.; Wack, F. X.; Hickel, R.; Greim, H. *Hum. Exp. Toxicol.* **1997**, *16*, 667.
8. Yoon, S.; Albers, A. E.; Wong, A. P.; Chang, C. J. *J. Am. Chem. Soc.* **2005**, *127*, 16030.
9. Harris, H. H.; Pickering, I. J.; George, G. N. *Science* **2003**, *301*, 1203.
10. Brummer, O.; La Clair, J. J.; Janda, K. D. *Bioorg. Med. Chem.* **2001**, *9*, 1067.
11. Boening, D. W. *Chemosphere* **2000**, *40*, 1335.
12. Descalzo, A. B.; Martinez-Manez, R.; Radeglia, R.; Rurack, K.; Soto, J. *J. Am. Chem. Soc.* **2003**, *125*, 3418.
13. Harano, K.; Hiraoka, S.; Shionoya, M. *J. Am. Chem. Soc.* **2007**, *129*, 5300.
14. Liu, B.; Tian, H. *Chem. Commun.* **2005**, 3156.
15. Ros-Lis, J. V.; Marcos, M. D.; Martinez-Manez, R.; Rurack, K.; Soto, J. *Angew. Chem. Int. Ed.* **2005**, *44*, 4405.
16. Prodi, L.; Bargossi, C.; Montalti, M.; Zaccheroni, N.; Su, N.; Bradshaw, J. S.; Izatt, R. M.; Savage, P. B. *J. Am. Chem. Soc.* **2000**, *122*, 6769.
17. Nolan, E. M.; Lippard, S. J. *J. Am. Chem. Soc.* **2003**, *125*, 3418.
18. Liu, J.; Lu, Y. *Angew. Chem. Int. Ed.* **2007**, *46*, 7587.
19. Ono, A.; Togashi, H. *Angew. Chem. Int. Ed.* **2004**, *43*, 4300.
20. Chiang, C.-K.; Huang, C.-C.; Liu, C.-W.; Chang, H.-T. *Anal. Chem.* **2008**, *80*, 3716.
21. Chen, P.; He, C. *J. Am. Chem. Soc.* **2004**, *126*, 728.
22. Fan, L.-J.; Zhang, Y.; Jones, W. E. *Macromolecules* **2005**, *38*, 2844.
23. Li, T.; Wang, E.; Dong, S. *Chem. Commun.* **2009**, 580.
24. Li, T.; Wang, E.; Dong, S. *Chem. Commun.* **2008**, 3654.
25. Li, D.; Wieckowska, A.; Willner, I. *Angew. Chem. Int. Ed.* **2008**, *47*, 3927.
26. Liu, X.; Tang, Y.; Wang, L.; Zhang, J.; Song, S.; Fan, C.; Wang, S. *Adv. Mater.* **2007**, *19*, 1471.
27. Kim, I. B.; Bunz, U. H. F. *J. Am. Chem. Soc.* **2006**, *126*, 728.
28. Xue, X.; Wang, F.; Liu, X. *J. Am. Chem. Soc.* **2008**, *130*, 3244.
29. Lee, J.-S.; Han, M. S.; Mirkin, C. A. *Angew. Chem. Int. Ed.* **2007**, *46*, 4093.
30. Kong, R.-M.; Zhang, X.-B.; Zhang, L.-L.; Jin, X. Y.; Huan, S.-Y.; Shen, G.-L.; Yu, R.-Q. *Chem. Commun.* **2009**, 5633.
31. Genereux, J. C.; Barton, J. K. *Chem. Rev.* **2010**, *110*, 1642.
32. Lincoln, P.; Norden, B. *Chem. Commun.* **1996**, 2145.
33. Tuite, E.; Lincoln, P.; Norden, B. *J. Am. Chem. Soc.* **1997**, *119*, 239.
34. Choi, M. S.; Yoon, M.; Baeg, J.-O.; Kim, J. *Chem. Commun.* **2009**, 7419.
35. Friedman, A. E.; Chambron, J.-C.; Sauvage, J.-P.; Turro, N. J.; Barton, J. K. *J. Am. Chem. Soc.* **1990**, *112*, 4960.
36. Murphy, C. J.; Arkin, M. R.; Ghatlia, N. D.; Bossmann, S. H.; Turro, N. J.; Barton, J. K. *Science* **1993**, *262*, 1025.
37. Ono, A.; Cao, S.; Togashi, H.; Tashiro, M.; Fujimoto, T.; Machinami, T.; Oda, S.; Miyake, Y.; Okamoto, A.; Tanaka, Y. *Chem. Commun.* **2008**, 4825.
38. Tanaka, Y.; Oda, S.; Yamaguchi, H.; Kondo, Y.; Kojima, C.; Ono, A. *J. Am. Chem. Soc.* **2007**, *129*, 244.
39. Li, T.; Li, B.; Wang, E.; Dong, S. *Chem. Commun.* **2009**, 3551.
40. Wang, Z.; Lee, J. H.; Lu, Y. *Chem. Commun.* **2008**, 6005.
41. Hiort, C.; Lincoln, P.; Norden, B. *J. Am. Chem. Soc.* **1993**, *115*, 3448.